Quantifying the variability of a complex ore using geometallurgical domains

Glacialle Tiu [a,*], Yousef Ghorbani [b], Nils Jansson [a], Christina Wanhainen [a], Nils-Johan Bolin [c]

[a] *Geosciences and Environmental Engineering, Swedish School of Mines, Dept. of Civil, Environmental and Natural Resources Engineering, Luleå University of Technology, SE-97187 Luleå, Sweden*
[b] *Joseph Banks Laboratories, University of Lincoln, LN6 7DL Lincolnshire, United Kingdom*
[c] *Boliden Mineral AB, SE-93632 Boliden, Sweden*

A B S T R A C T

This comprehensive study focuses on the geometallurgical characterization of the complex Lappberget poly-metallic Zn-Pb-Ag-(Cu-Au) sulfide deposit at the Garpenberg mine, one of Sweden's largest and most significant sources of zinc, lead, and silver. The research explores the intricate mineralogy and texture of the ore, investigating its impact on the variability of flotation performance for different ore types. QEMSCAN® analysis and element-to-mineral conversion (EMC) were employed to quantitatively characterize the ore in terms of mineral distribution and occurrence. The study revealed significant variability in Cu-Pb flotation compared to Zn flotation due to the targeted mineral varieties. While zinc primarily occurred in sphalerite grains, Cu-Pb flotation aimed to recover multiple Pb-, Cu-, Ag- and Au-bearing minerals that were finely grained and intricately intergrown with other sulfides. Grain size and the degree of liberation emerged as primary rate-limiting factors, especially in the Zn flotation circuit. Seven geometallurgical domains were defined based on the concentration efficiencies (i.e., selectivity and recovery) for sphalerite, galena, chalcopyrite, and Ag-bearing phases. The proposed geometallurgical characterization approach aims to transform geologically defined classes into geo-metallurgical domains by relating the deposit's key mineralogical and textural characteristics to metallurgical performance.

1. Introduction

Variability, or heterogeneity, is an inherent characteristic of all geological objects, features, and processes. This variability can be constrained by the controlling geological elements of a deposit, such as lithological and alteration boundaries, structure, and the distribution of grades and other attributes. These factors are often incorporated when creating geological models and defining a mineral resource (Kopacz et al., 2020; Spleit and Dimitrakopoulos, 2017). Quantifying the heterogeneity of a deposit is typically done using geological domains, which are defined using the rock's geological attributes, such as mineralogy, lithology, and alteration (Boroh et al., 2021). Consequently, this variability can also result in variations in the quality of the feed to a mineral processing plant, posing a major challenge for mineral processing operations. However, the geological-mineral processing relationship often remains unclear due to the limited availability of fit-for-purpose process mineralogical data (Ehrig et al., 2014; Williams and Richardson, 2004).

Geometallurgy is a cross-disciplinary science that integrates geological and metallurgical information necessary for the planning and management of mining operations. Geometallurgy aims to predict the plant performance by understanding the relationship between the ore's geological characteristics and its processability (Lamberg et al., 2013; Lishchuk, 2016; Lishchuk et al., 2020). Similar to geological domains, geometallurgical domains can help constrain the metallurgical variability within a deposit by identifying units with similar mineralogy, texture, and composition, which are expected to have similar metallurgical performance (Johnson and Munro, 2008). These units can be defined using chemical assays (traditional approach) or through mineralogical characterization. The latter approach has been successfully employed for mostly iron and copper–gold ores (e.g., Bahrami et al., 2021; Lund, 2013; Martino et al., 2016; Rajabinasab and Asghari, 2019; Tijsseling et al., 2020). However, few studies have been conducted in the geometallurgical modeling of complex ores, such as those that

---

* Corresponding author.
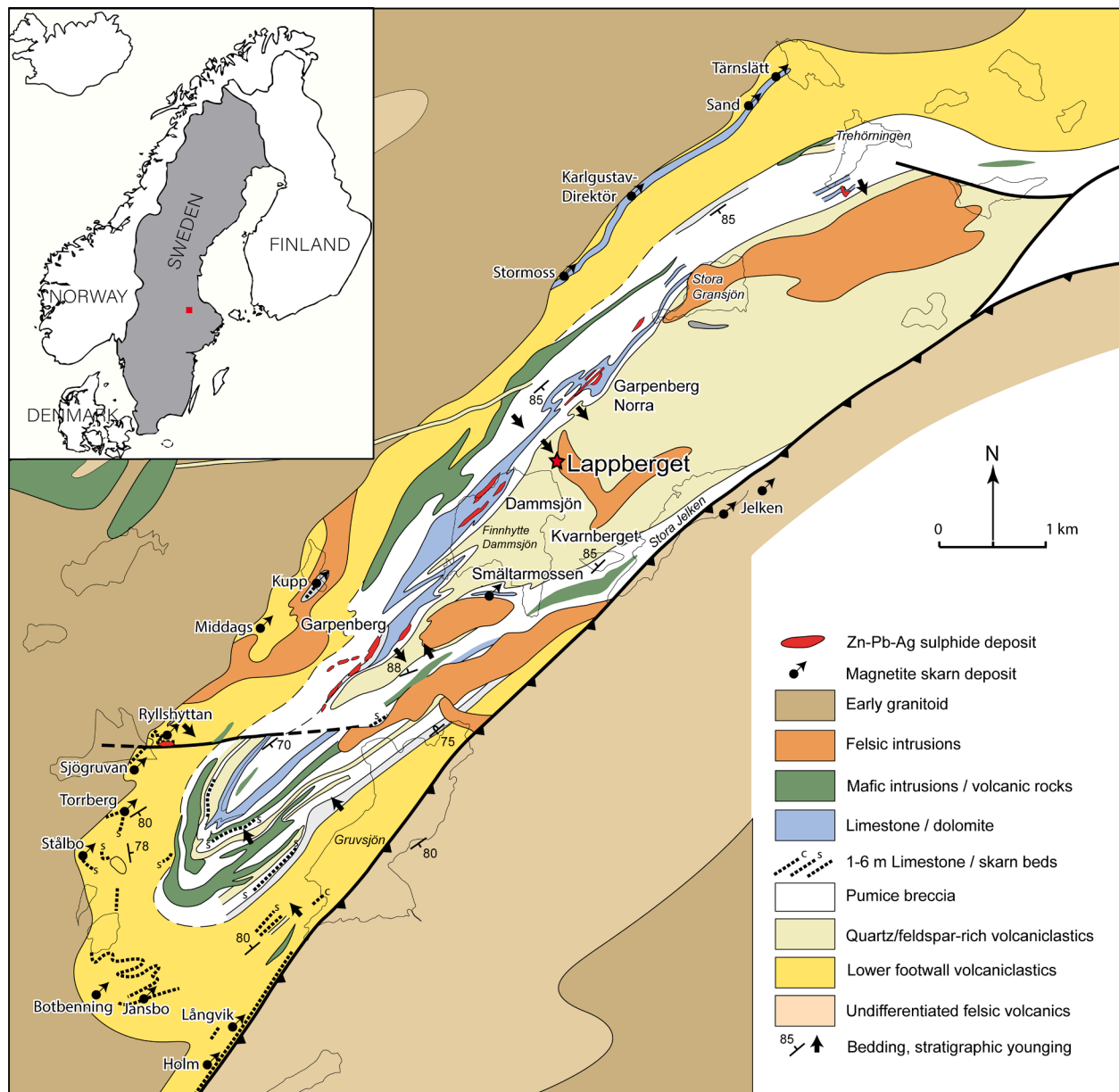 *E-mail address:* glacialle.tiu@ltu.se (G. Tiu).

Fig. 1. Regional geological map of the Garpenberg area with inset showing its location (red square) (modified from Allen et al., 2003). (For interpretation of the references to colour in this figure legend, the reader is referred to the web version of this article.)
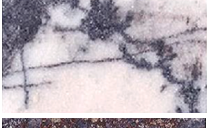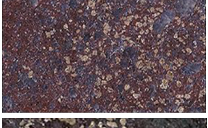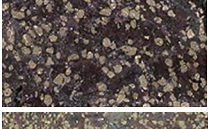
produce three or more metals (e.g., Alruiz et al., 2009; Bevandic, 2022; Gordon, 2019; Minz et al., 2013; Olarewaju et al., 2015; Suazo et al., 2010). These deposits are harder to predict due to the large number of variables affecting the plant performance and recoveries. In addition, there are multiple processing streams with unique technical characteristics, which should be considered.

In this study, the Lappberget Zn-Pb-Ag-(Cu-Au) sulfide deposit was selected as a case study to investigate the use of mineralogy-based geometallurgical domaining to quantify the metallurgical variability within the deposit. The Lappberget deposit is currently mined to produce four concentrates: zinc, lead, copper, and a gravimetric concentrate targeted for gold and silver through sequential Cu-Pb-Zn flotation. Variability in the feed grade and recovery in the concentrator has been reported as one of the major challenges for the processing plant. In most cases, process operators need to adjust the operational parameters on a case-by-case basis when poor process performance is observed, such as changes in grade or froth instability. Unless the reasons for such variability are clearly understood and accounted for, incremental

improvements to the process performance can be easily overwhelmed by the variability in the feed. Geological characterization of the Lappberget deposit by Tiu et al. (2021) identified seven different mineralization styles within the deposit, for which chemical, textural and mineralogical variability was observed: (1) magnetite mineralization, (2) skarn-hosted sulfide mineralization, (3) carbonate-hosted Ag-rich galena veinlets, (4) massive Zn-Pb sulfide mineralization, (5) chalcopyrite-rich massive Zn-Pb sulfide mineralization, (6) mineralized shear zones, and (7) footwall disseminated to semi-massive mineralization. The mineralization styles are linked to litho-structural boundaries that are refined by mineral distribution patterns.

This paper aims to determine if the metallurgical variability in the deposit can be quantified by using geologically defined domains as a basis for geometallurgical sampling, testing, and characterization. To do this, representative drill core samples were selected from each domain and subjected to laboratory-scale bulk sulfide flotation tests. Mineralogical and particle information was collected on the flotation products for each domain using automated mineralogy (QEMSCAN®, Gottlieb

Table 1
Mineralogical and textural characteristics of the different ore classes identified in this study. All drill core photos are of the same scale.

	Mineralization styles	Drill core photo	Geological Domains	Major sulfides	Major gangue	Character and ore texture
Upper ore body	Magnetite mineralization (Mt)		Quartz-magnetite-skarn mineralization (QMt)	py > sp > gn > po	qtz, px, amp, grt, cal, mt	presence of fine to coarse-grained magnetite occurring in stringers and in veins, enriched in Ag and Sb minerals; hosted in highly silicified rocks
	Skarn-hosted sulfide mineralization (SKN)		Skarn-hosted ore (SKN)	py > sp > gn	amp, px, dol, chl, tlc, cal, mca	composed mainly of amphiboles with minor presence of talc and interstitial medium to coarse grained sphalerite and galena
	Carbonate-hosted Ag-rich sulfide-sulfosalt veinlets (AgD)		Dolomite-hosted ore (DOL)	py > sp > gn	dol, cal, px	argentiferous galena veinlets hosted in manganoan dolomitic and calcitic rocks; coarser-grained galena veins present (rare) and associated with quartz veins
Main ore body	Massive sphalerite-pyrite-galena mineralization (MSPG)		Massive sp-py-gn mineralization (MSPG)	sp > py > gn	qtz, amp, px, mca, cal, dol	consists of a medium- to coarse- grained sphalerite-galena matrix and wall rock and pyrite fragment clasts; hosted in a highly silicified rock
			Mn-rich massive sp-py-gn mineralization (MnMSPG)	sp > py > gn	qtz, dol, cal, amp, px, grt	similar to MSPG but hosted in manganoan dolomite/skarn
			Pyrite-rich massive sulfide mineralization (MPSG)	py > sp > gn > po	amp, dol, qtz, px, fsp, grt, chl	similar to MSPG but has higher pyrite content with finer-grained matrix; hosted by silicified actinolite-tremolite skarn
	Massive sphalerite-galena-pyrite-chalcopyrite-pyrrhotite ± Au mineralization (MSGC)		Chalcopyrite-bearing massive sulfide mineralization (MSGC)	sp > gn > py≫ ccp	qtz, fsp, mca, amp	similar to MSPG but higher galena and less pyrite content, chalcopyrite also occurs (albeit minor); hosted in mica quartzite
	Mineralized shear zones (MSZ)		Talc-bearing sulfide mineralization (TLC)	py > sp > gn	qtz, amp, tlc, px	composed mainly of talc and skarn minerals; associated with shear zones
Lower ore body	Footwall disseminated mineralization (FWD)		Muscovite-quartz hosted ore (MQ)	py > sp > gn	qtz, mca, fsp	sulfide mineralization typically occurs as disseminations and elongated parallel to the foliation; hosted in muscovite-rich mica quartzite
			Biotite-quartz hosted ore (BQ)	py > sp > gn≫ ccp	qtz, mca, fsp	sulfide mineralization typically occurs as disseminations and elongated parallel to the foliation; has minor chalcopyrite content; hosted in biotite quartzite/schist

amp - amphibole; cal - calcite; chl- chlorite; ccp - chalcopyrite; dol - dolomite; fsp - feldspar; gn - galena; grt - garnet; mca - mica; po - pyrrhotite; py - pyrite; px - pyroxene; sph - sphalerite; tlc - talc; qtz - quartz.

et al., 2000), augmented by data obtained from chemical analysis. Geometallurgical domains were defined based on the variability in the flotation response of the different geological domains. A geometallurgical characterization approach was proposed, which aims to use geological data to better understand and predict the metallurgical variability of the deposit and to guide future data collection toward parameters that are most relevant to the flotation process.

1.1. Geological setting

Lappberget is a stratabound Zn-Pb-Ag-(Cu-Au) deposit within the Garpenberg mine, located approximately 180 km northwest of Stockholm, Sweden. The Lappberget deposit is currently the largest known sulfide deposit in the mine, with a combined mineral resource and mineral reserve of 72.9 Mt at 2.86% Zn, 1.12% Pb, 0.05% Cu, 66 g/t Ag, and 0.40 g/t Au (Derrien, 2022). The deposit is located on the northwest limb of the Garpenberg syncline, along with several other Zn-Pb-Ag sulfide deposits (Fig. 1).

Ore host rocks are composed of intensely altered and metamorphosed felsic volcanic rocks and former limestone interbeds that are overlain by less altered metavolcanic rocks. The stratigraphic footwall rocks consist of highly silicified and/or micaceous rocks inferred as
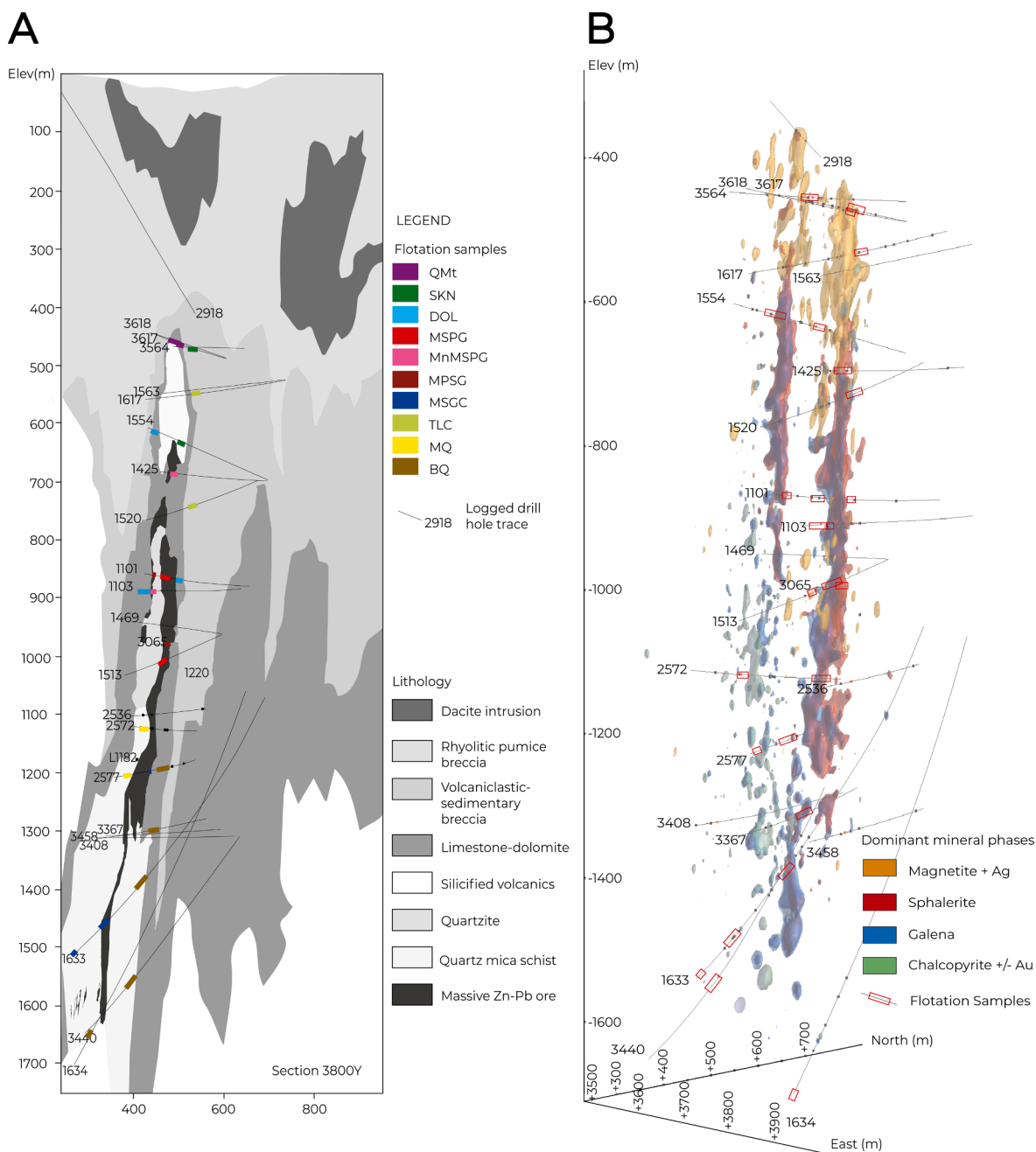
Fig. 2. Sample locations plotted in the (A) geological cross-section and (B) 3D mineralogical model of the Lappberget deposit. For complete sample names, see Table 1.

massive to bedded metavolcanic rocks of rhyolitic to dacitic and subordinately basaltic composition (Jansson and Allen, 2011). This sequence is overlain by the main sulfide ore host, which consists of a skarn unit and calcitic to dolomitic marble. Less altered, metamorphosed, rhyolitic to basaltic volcanic breccia, conglomerates, and sandstones with subvolcanic dacitic intrusion characterize the stratigraphic hanging wall rocks. Sphalerite, galena, and pyrite are the main sulfide minerals, whereas pyrrhotite and chalcopyrite constitute minor components. Oxides such as magnetite are mainly found in the upper portion of the deposit. Ore minerals occur as massive ores, disseminations, veinlets, breccia-infills, and vein networks.

2. Material and methods

2.1. Sample selection

The geological domains were defined based on the seven mineralization styles identified by Tiu et al. (2021). The massive sulfide mineralization ore type was subdivided into three classes based on their spatial location with the main ore lens, host lithologies, and the relative abundance of pyrite, sphalerite, and galena. Similarly, the footwall disseminated rocks are divided into two based on the difference in the characteristics of their host lithology and sulfide abundance. The ten geological domains identified are summarized in Table 1.

Quartered drill core samples representing the ten geological domains were collected (approximately 20–60 kg for each ore type). Sample locations are plotted in Fig. 2. The drill core samples of each ore class were
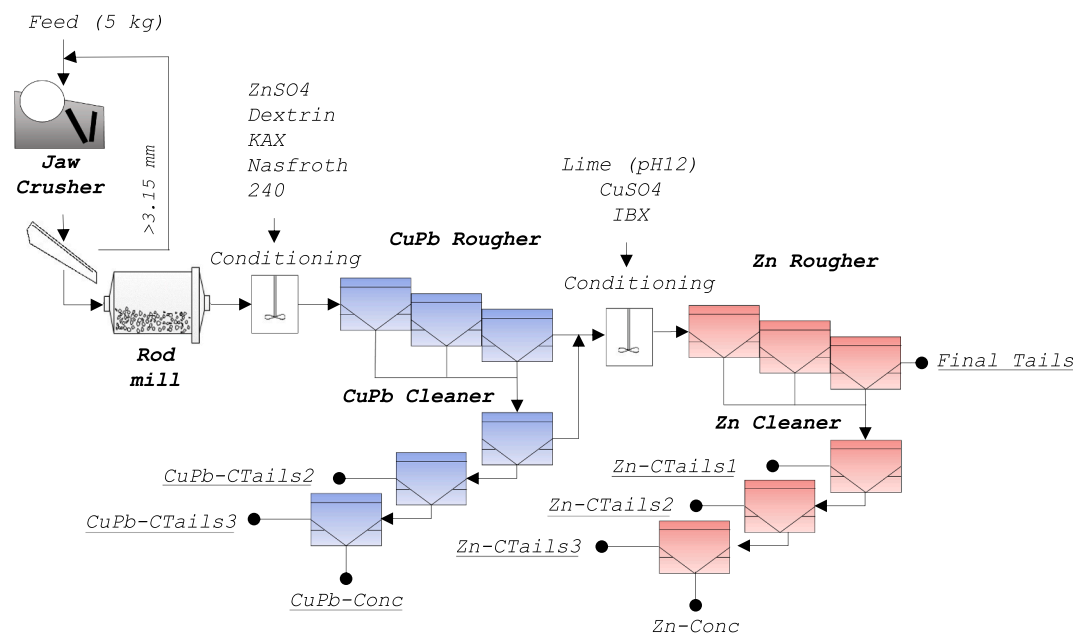
Fig. 3. Scheme for the flotation test for the ten Lappberget ore types. Flotation products are underlined.

Table 2
Operating conditions for the flotation test.

	Rougher stage	Cleaner stage
Cell type	Outotec (8 L)	WEMCO (2.7 L)
Stirring speed (rpm)	900	300
Scraping time (sec)	0.4	Manual
Air flow rate (NL/min)	5	not measured
% Solids (wt%)	45*	not measured
pH	12**	not measured
Reagents	*Cu-Pb Rougher*	*Zn Rougher*
Collector	PAX (potassium amyl xanthate)	IBX (isobutyl xanthate)
Frother	Nasfroth 240 (polyethylene glycol monobutyl ether)	
Depressant	ZnSO$_4$ and Dextrin (yellow)	
Activator		CuSO$_4$
pH Regulator		Slaked lime (Ca (OH)$_2$)

* Estimated for 5 kg feed for 8L cell.
** only regulated during the Zn rougher flotation.

Table 3
Description of each flotation product.

Flotation product	Description
CuPb-Conc	Cu-Pb concentrate
CuPb-CTails2	Cu-Pb 2nd cleaning stage tails
CuPb-CTails3	Cu-Pb 3rd cleaning stage tails
Zn-Conc	Zn concentrate
Zn-CTails1	Zn 1st cleaning stage tails
Zn-CTails2	Zn 2nd cleaning stage tails
Zn-CTails3	Zn 3rd cleaning stage tails
FinalTails	Tailing from the Zn Rougher unit

crushed to less than 3.15 mm using a jaw crusher, followed by mixing and homogenization. The samples were then split into 1 kg samples using a rotary sample splitter.

2.2. Flotation test

Standard batch flotation tests were carried out for samples from the ten ore types; the purpose was to compare the flotation response of each ore type. Five 1 kg bags from the crushed drill cores were combined to create the feed for each flotation test. The 5 kg feed was ground for 45

min in a rod mill (i.e., Sala torque mill with a diameter of 280 mm and a length of 440 mm) with 2.7 L of water and 49 kg stainless steel rods mill charge with diameters between 5 and 25 mm. The mill was rotated at 54 rpm.

The scheme for the flotation tests was designed based on the standard regime used by Boliden Mineral AB for the Garpenberg mine. Fig. 3 illustrates the workflow for the flotation tests conducted under the operating conditions in Table 2. Two flotation tests were conducted for each of the ten different ore types.

Eight flotation products were collected for each test, as listed in Table 3. The flotation products were dried, weighed, and prepared for analysis in Boliden's mineral processing laboratory.

2.3. Characterization of the flotation products

All the flotation products from the two tests were split into two sample sets. The first set was submitted to Intertek Genalysis Laboratory in Australia following the methodologies described in Intertek (2020). The reference number of procedures used are: FA25/OE04 (Au), 4A/MS48 (48 elements), 4AO/OM (samples with grade exceeding detection limits for Cu, Zn, Pb, and S of MS48 procedure), 4A-ICPMS (Hg), FP6/OM (high-grade Ag and Pb). For all the repeat flotation tests, the second set of samples was sized using 45- and 63-μm sieves to create three size fractions. 30-mm polished resin mounts were prepared for the different size fractions for optical microscopy and QEMSCAN® analysis.

Petrographic investigations were carried out using optical light microscopy (Nikon ECLIPSE E600 POL, Luleå University of Technology). Modal mineralogy and particle characteristics of the Zn-Conc, CuPb-Conc, and FinalTails for all ore types were analyzed using QEMSCAN® 650 (FEI with W-filament, two EDS, and an electron backscatter detector) at Boliden's mineral processing laboratory. The particle mineralogical analysis (PMA) measurement mode was performed with an emission current of 10nA and an accelerating voltage of 25 kV. The species identification protocol (SIP) or mineral library used to discriminate minerals was modified based on the mineralogical characterization and composition by Tiu et al. (2021). FEI™ iMeasure version 5.4 and iDiscover 5.4 software were used for data collection and processing. Grain size is measured based on the equivalent spherical diameter (ESD) extracted from the QEMSCAN® analysis.
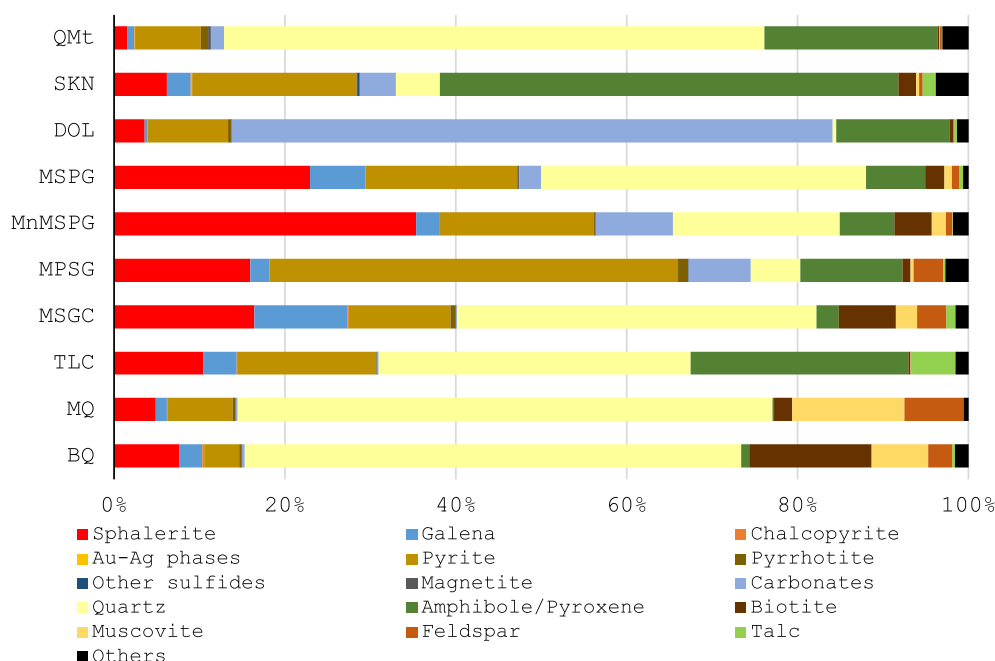
Fig. 4. Calculated bulk modal mineralogy from QEMSCAN® analysis of samples from the ten geological domains.

Element-to-mineral conversion (EMC), described in Whiten (2007), was used to determine the modal mineralogy of the cleaner tails products (i.e., CuPb-Tails2, CuPb-Tails3, Zn-Tails1, Zn-Tails2, Zn-Tails3). The modal mineralogy of the feed was back-calculated from all the flotation products. The mineral composition matrix utilized for the EMC calculations is based on the mineralogical study by Tiu et al. (2021) (see Supplementary Material Tables 1 and 2). Mineral ratios based on the QEMSCAN® analysis of each ore type were utilized to constrain the matrix calculations. The comparison between the mineral distribution calculated by the EMC method and the QEMSCAN® analysis showed a high level of agreement for the major and minor minerals but not for

trace minerals (see Supplementary Material Fig. 1).

2.4. Concentration efficiency

There are several methods to assess and quantify the effectiveness of the concentration operations (e.g., Metallurgical Efficiency (Diamond and Trail, 1927), Selectivity Index (Gaudin and Butte, 1930), Absolute Efficiency (Luyken and Bierbrauer, 1929)). This study utilizes the Concentration Efficiency (E_c) as defined by Stevens and Collins (1961). Unlike other separation efficiency indexes, which are mainly based on the recovery of minerals and rejection of gangue, E_c is a product of

Table 4

Mineral abundance of host minerals in wt% for zinc, lead, copper, silver, and gold for the different ore types. Mineral formulas are based on Tiu et al. (2021).

	Mineral phase (abbreviation)	Mineral Formula	Upper ore body			Main Ore body					Lower ore body	
			QMt	SKN	DOL	MSPG	MnMSPG	MPSG	MSGC	TLC	MQ	BQ
Zn	Sphalerite[a]	$Zn_{0.8-1.08}Fe_{0-0.2}Mn_{0-0.1}S$	2.07	9.79	4.52	23.43	23.69	16.69	19.79	10.48	6.88	8.84
	Gahnite	$ZnAl_2O_4$[a]	*	*	*	*	*	*	*	*	*	0.02
Pb	Galena	PbS	0.70	2.66	0.86	6.45	3.55	2.23	10.01	2.59	1.78	2.63
	Boulangerite	$Pb_5Sb_4S_{11}$[a]	*	*	*	*	*	*	*	*	*	*
	Jordanite	$Pb_{13.8-13.9}(As_{4.6-5}Sb_{1.1-1.3})S_{23-23.1}$	*	*	*	*	*	*	*	*	*	*
	Bournonite[b]	$PbCuSbS_3$	*	0.01	*	*	*	*	*	*	*	*
	Diaphorite[c]	$Pb_2Ag_3Sb_3S_8$[a]	*	*	*	*	*	*	*	*	*	*
Cu	Chalcopyrite	$CuFeS_2$	0.04	0.28	0.08	0.13	0.61	0.13	0.84	0.12	0.11	0.69
	Cubanite	$CuFe_2S_3$	0.01	0.02	0.01	0.01	*	0.01	0.04	0.01	0.01	0.03
	Freibergite[c,d]	$(Cu_{4.3-10.6}Ag_{0.1-6.2}Zn_{0-1.1}Fe_{0.1-2}Mn_{0-1.9})(Sb_{0.2-4.2}As_{0-3.8})S_{12.2-13.6}$	0.01	0.03	*	0.01	*	*	*	0.01	*	*
	Tetrahedrite[c,d]		*	0.04	*	*	*	*	0.02	*	*	*
	Tennantite[c,d]		*	*	*	*	*	*	*	*	*	*
Ag	Native Silver	Ag	0.01	0.01	*	*	*	*	*	*	*	*
	Allargentum	$Ag_{0.81-0.98}Sb_{0.01-0.15}$	0.01	*	*	*	*	*	*	*	*	*
	Dyscrasite	$Ag_{3.1-3.2}Sb_{0.8}$	*	*	*	*	*	*	*	*	*	*
	Acanthite	Ag_2S[a]	*	*	*	*	*	*	*	*	*	*
	Pyrargyrite	Ag_3SbS_3[a]	*	*	*	*	*	*	*	*	*	*
Au	Electrum[c]	(Au,Ag)[f] 10-87 wt% Ag	*	*	*	*	*	*	*	*	*	*
	Pyrite[a]	FeS_2	6.84	11.85	5.53	10.25	14.11	10.46	7.00	23.79	4.82	8.66

[a] contains trace amounts of Au.
[b] also a Cu host mineral.
[c] Ag host mineral.
[d] Zn host mineral.
[e] based on stoichiometric formula (Anthony and Bideaux, R.A., Bladh, K.W., Nichols, 1990).
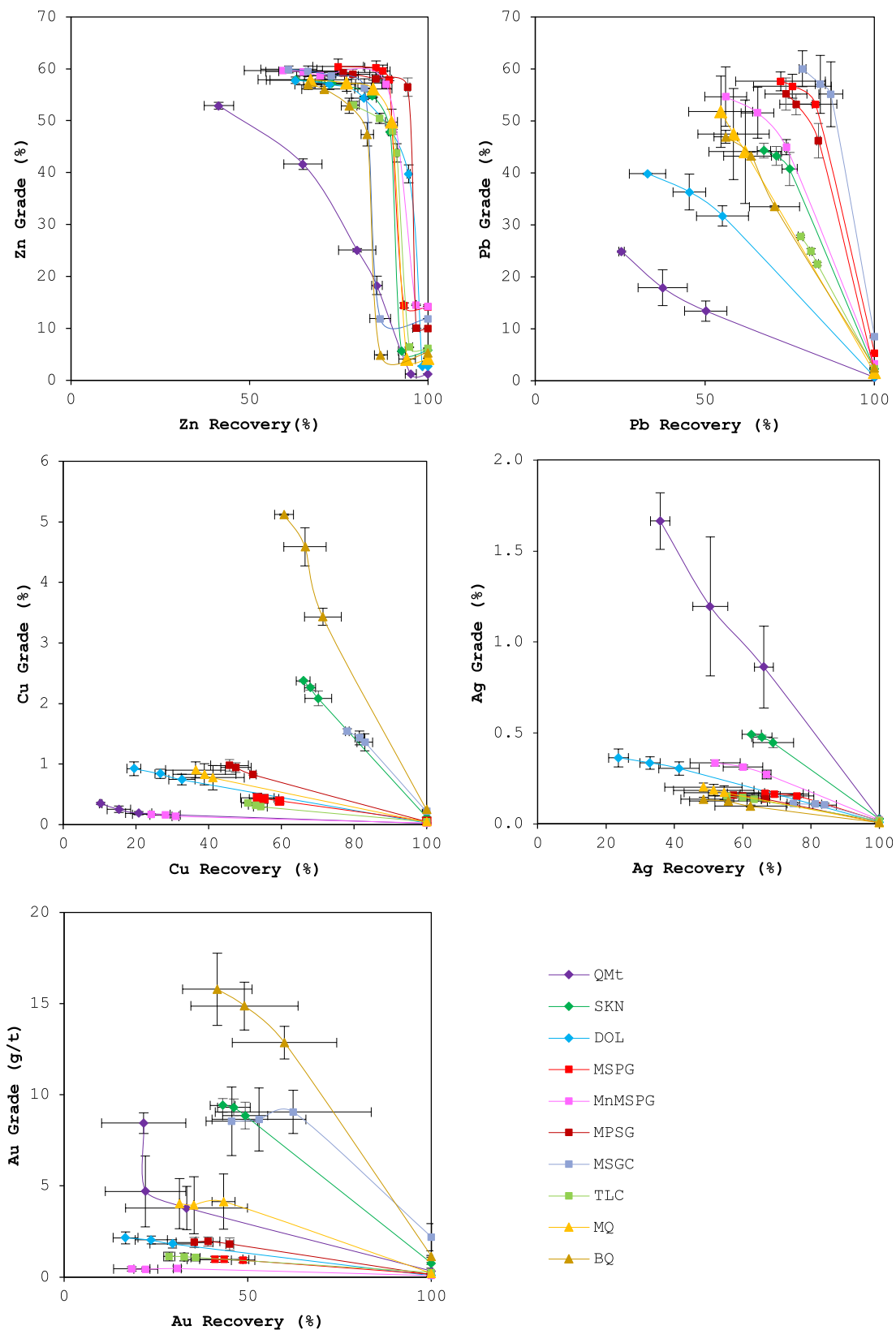[f] not a mineral but an alloy, *trace amount(<0.01 wt%).

Fig. 5. Grade and recovery plots for the different ore classes based on the average values from the two flotation tests. Range bars indicate the values from the repeat flotation tests.
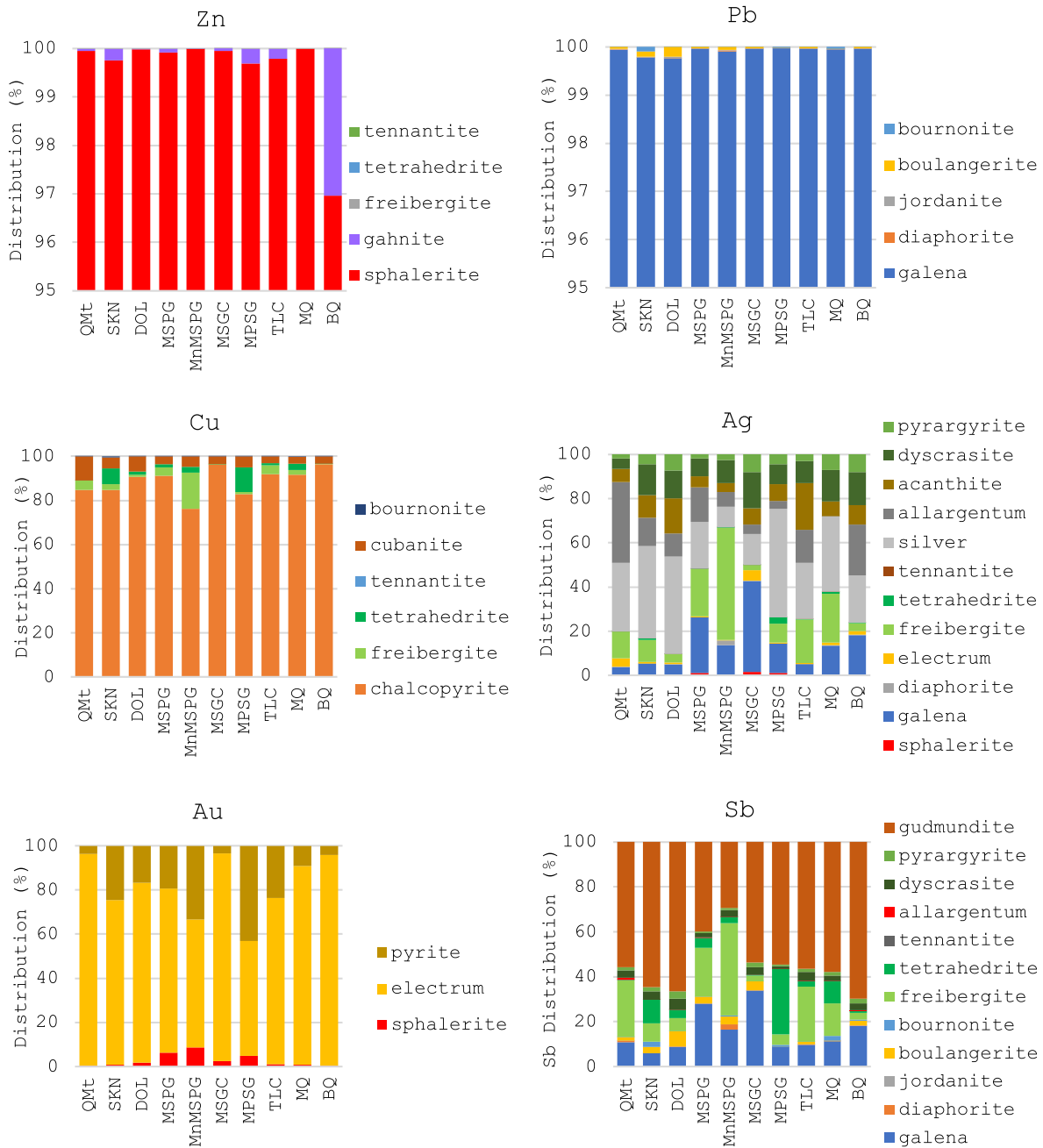
Fig. 6. Metal deportment for Zn, Pb, Cu, Ag, Au, and Sb for the different ore types. For Zn and Pb graphs, the distribution (%) ranges from 95 to 100.

recovery and selectivity. It is suitable for assessing the separation efficiency between different ores while minimizing the effect of head grades. E_c is defined as:

$$E_c = \frac{(c - f)}{(c_{max} - f)} \times R \qquad (1)$$

where c is the concentrate grade, f is the feed grade, c_{max} is the maximum concentrate grade obtainable at 100% recovery (e.g., element grade in the mineral being concentrated), and R is the percent recovery. In terms of mineral grades and recoveries, E_c is calculated as:

$$E_{c_m} = \frac{(c_m - f_m)}{(100 - f_m)} \times R_m \qquad (2)$$

E_c values range from 0 to 100%, with a maximum value of 100% corresponding to a perfect separation resulting in 100% recovery at 100%

grade (i.e., for mineral separation). In this study, E_c was calculated for sphalerite, galena, chalcopyrite, and Ag-bearing phases (incl. freibergite, tetrahedrite, native silver, acanthite, allargentum, dyscrasite, and pyrargyrite).

The flotation performance of the ten geological domains was compared. One-way analysis of variance (ANOVA) using Minitab® was used to determine whether there is a significant difference between the E_c values for sphalerite, galena, chalcopyrite, and Ag-bearing phases for the different domains. Fisher's Least Significant Difference (LSD) method was used for creating pairwise comparisons for each domain (Triola, 2018). Given the limited data (i.e., two repeat tests), it was assumed that there is equal within-group variance across the groups. The results from this comparison will serve as a guideline for defining the geometallurgical domains.
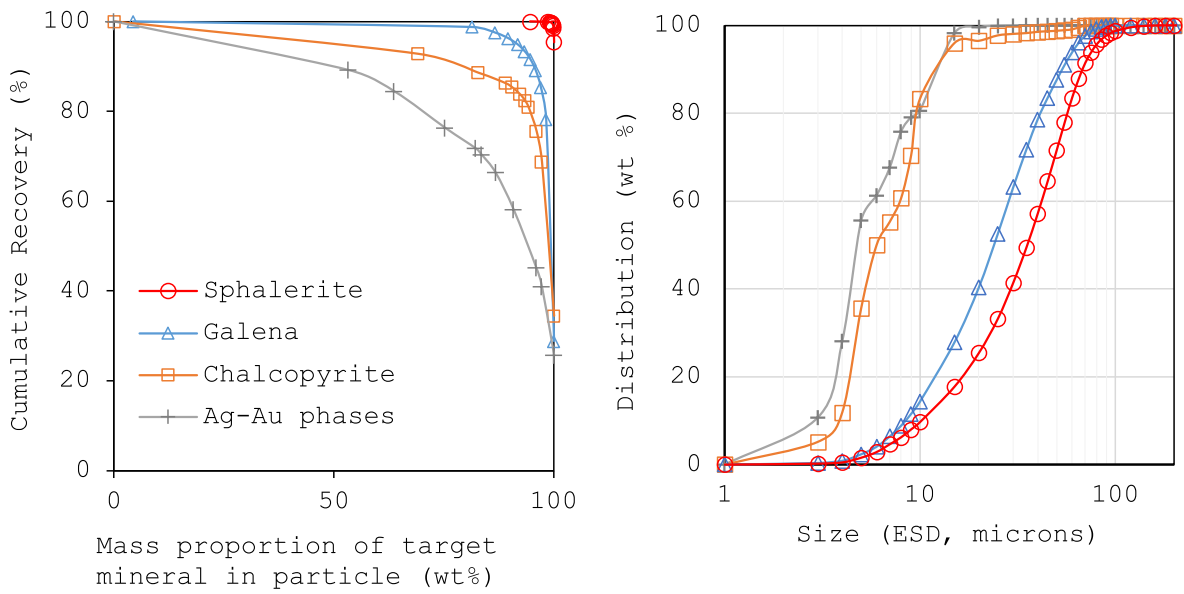
Fig. 7. Liberation curves (left) and grain size distribution (right) of sphalerite, galena, chalcopyrite, and Au-Ag phases for MSPG.

3. Results and discussion

3.1. Mineralogical composition

Distinct mineralogical differences are observed for most ore classes (Fig. 4). The massive sulfide ore types (MSPG, MnMSPG, MPSG, and MSGC) contain>40% sulfides. Except for MPSG, sphalerite is the most dominant sulfide within the massive sulfide ore classes, whereas pyrite is the most dominant for the other ore types. Quartz, amphibole, and carbonates (i.e., dolomite and calcite) are the most dominant non-
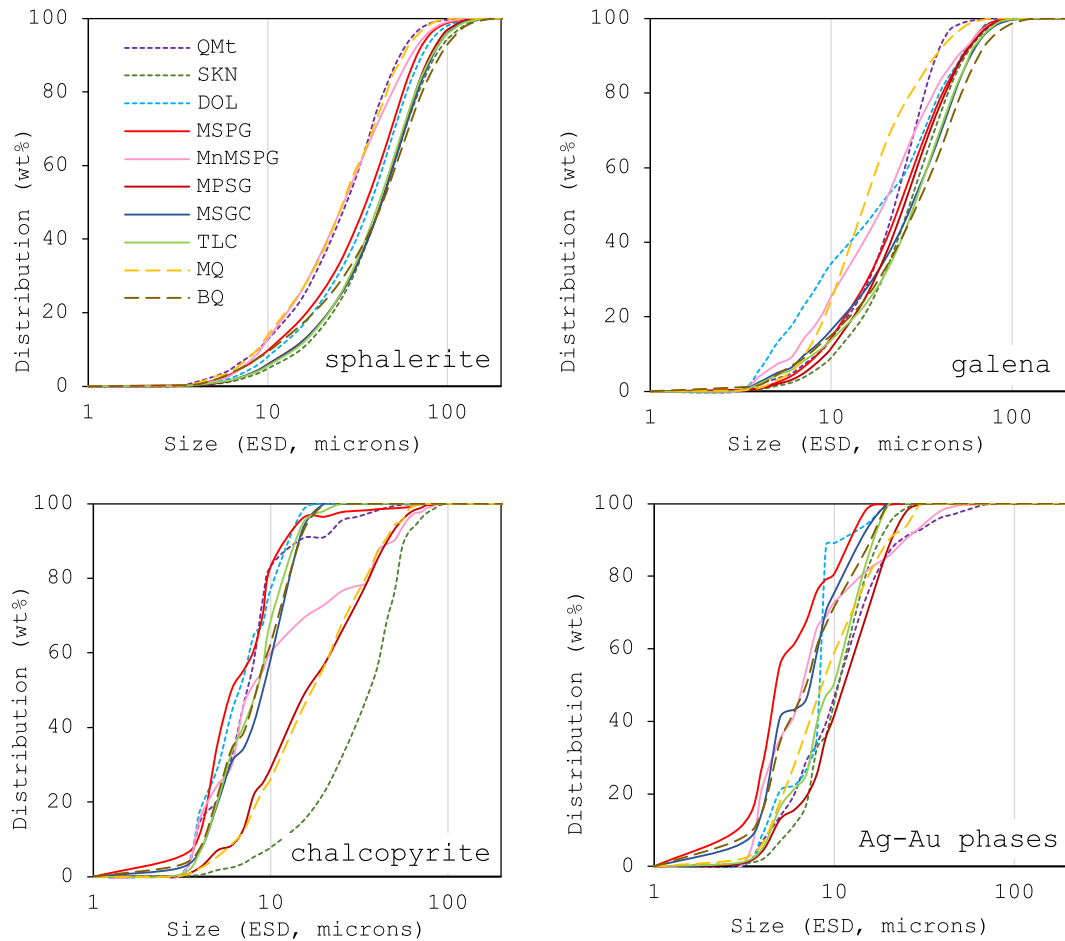

Fig. 8. Cumulative grain size distribution of sphalerite and galena based on equivalent spherical diameter (ESD) calculated from the QEMSCAN® analysis.
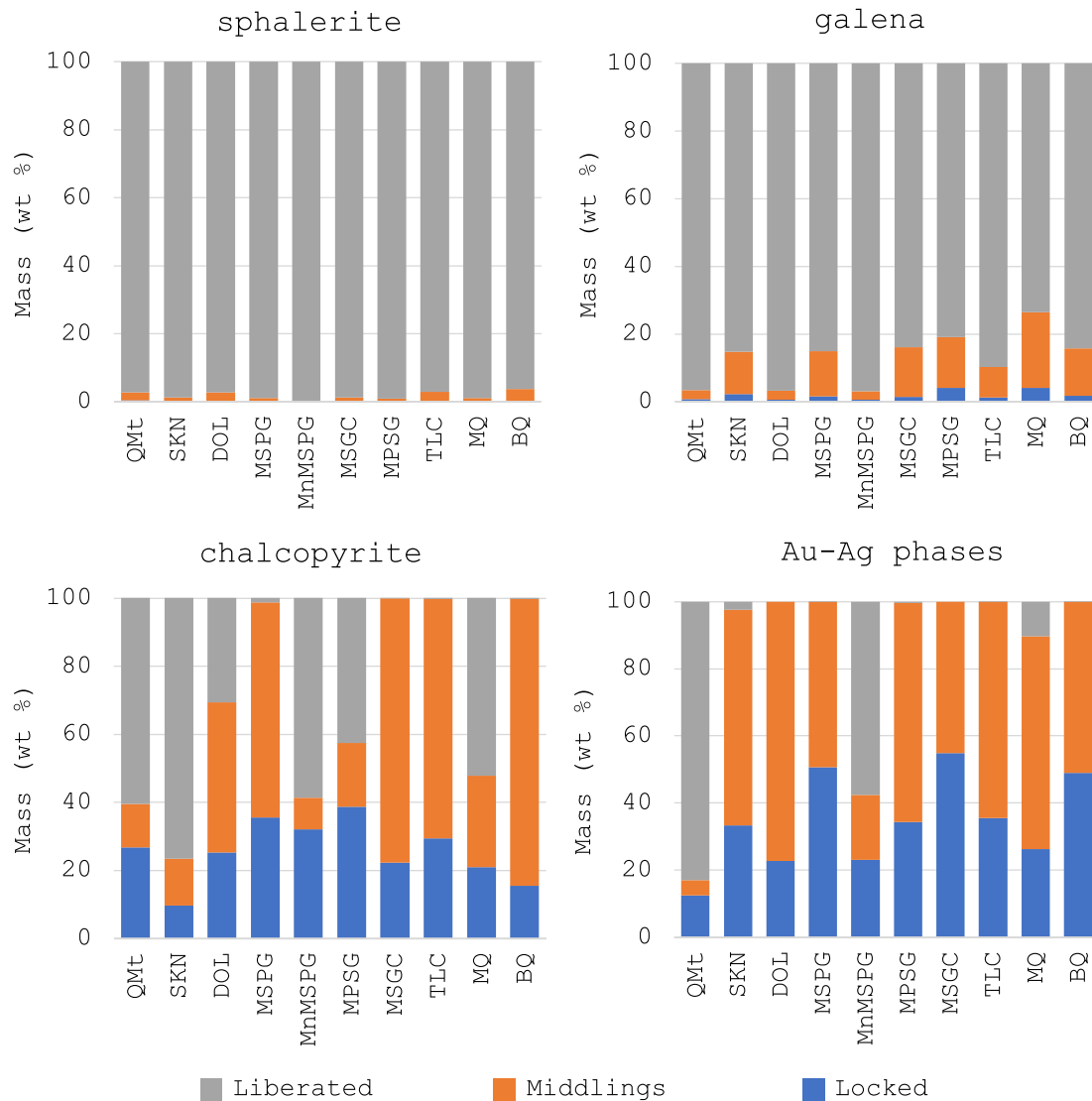
Fig. 9. Degree of liberation for economic sulfides from the QEMSCAN® analysis. Legend: Liberated (>80% degree of liberation), Middlings (20–80% degree of liberation), and Locked (<20% degree of liberation).

sulfide gangue minerals for all the ore classes. Silver is enriched in the ore types in the upper parts of the deposit (QMt and SKN), whereas copper and gold are highest for MSGC and BQ ore types, which are in stratigraphically lower parts of the deposit (Fig. 2).

A wide variety of minerals host the economic metals zinc, lead, copper, silver, and gold, as listed in Table 4. Sphalerite, galena, and chalcopyrite are the primary hosts for zinc, lead, and copper. Gahnite ($ZnAl_2O_4$) occurs in trace amounts except in BQ. Aside from galena, other Pb-phases only occur in trace amounts (<0.01 wt%). Cubanite ($CuFe_2S_3$) and freibergite-tetrahedrite series $(Cu,Ag,Fe,Mn)_{12}(Sb, As)_4S_{13}$ are secondary host minerals for copper. Silver mineralogy is more complex and varies between different ore types. Native silver and allargentum ($Ag_{1-x}Sb$) are the main Ag-bearing minerals, followed by freibergite, tetrahedrite, acanthite (Ag_2S), dyscrasite (Ag_3Sb), and pyrargyrite (Ag_2SbS_3). Galena (median = 0.08 wt% Ag) is also a significant Ag-bearing phase, especially for the massive ores. Gold is mainly present as an electrum alloy (Au, Ag). Pyrite and sphalerite secondarily contribute to the gold content in the deposit when accounting for the trace amount present in pyrite (median = 0.13 ppm) and sphalerite (median = 0.03 ppm). Antimony is strongly associated with silver and is generally present in most Ag-bearing minerals. Arsenic is mainly hosted in arsenopyrite and pyrite (median = 0.05 wt% As content).

3.2. Flotation performance

To evaluate the flotation performance of the different ore types, grade and recovery curves for Zn, Pb, Cu, Ag and Au are plotted in Fig. 5. Grade and recovery data for all flotation test is available in the Supplementary Material Table 3. The following information can be extracted from the plots:

- The grade and recovery curves for the zinc flotation, except for QMt, follow similar trends for all ore types.
- Cu-Pb flotation shows higher variability, i.e., in terms of grade and recovery (Cu, Pb, Ag, and Au) and concentration efficiency values for the different ore types.
- Pb flotation performance varies significantly between different ore types, wherein massive sulfide ores provide the highest grade and recovery.
- Overall, QMt samples have the poorest flotation performance (lowest recoveries) but have the highest silver grades.
- Within the massive ore types, MnMSPG has the poorest flotation performance.
- BQ, MSGC, and SKN show the highest copper and gold grade and recovery.
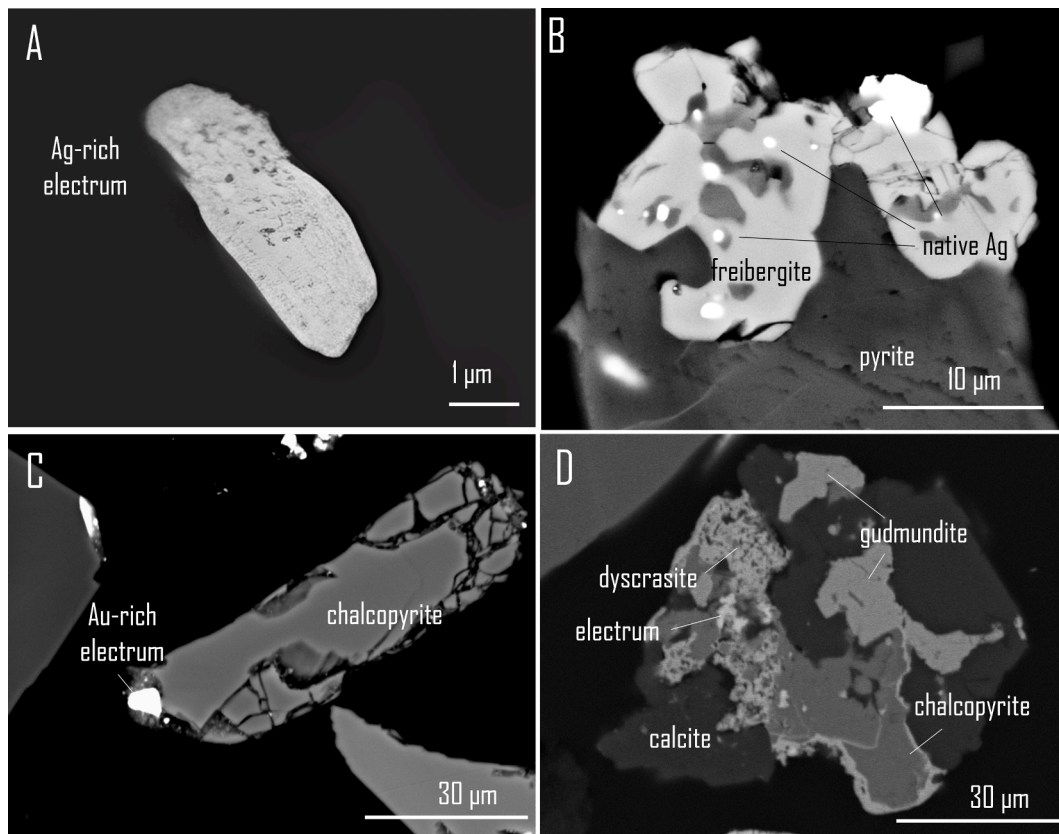
Fig. 10. Scanning electron microscope (SEM) images of Ag- and Au-bearing phases: (A) liberated Ag-rich electrum particle (QMt Final Tails), (B) native Ag as inclusions in freibergite intergrown with pyrite (QMt Final Tails), (C)Au-rich electrum attached in a chalcopyrite grain (BQ CuPb Conc), and (D) complexly inter-grown Ag-phases (dyscrasite and electrum) with chalcopyrite, gudmundite and calcite (BQ CuPb CTails3).

- Anomalous grade and recovery trends of gold for some samples are attributed to the nugget effect (e.g., MSGC flotation test 1 Cu-Pb cleaner concentrate has a higher grade than the final Cu-Pb concentrate).

The high variability in the performance of the Cu-Pb flotation
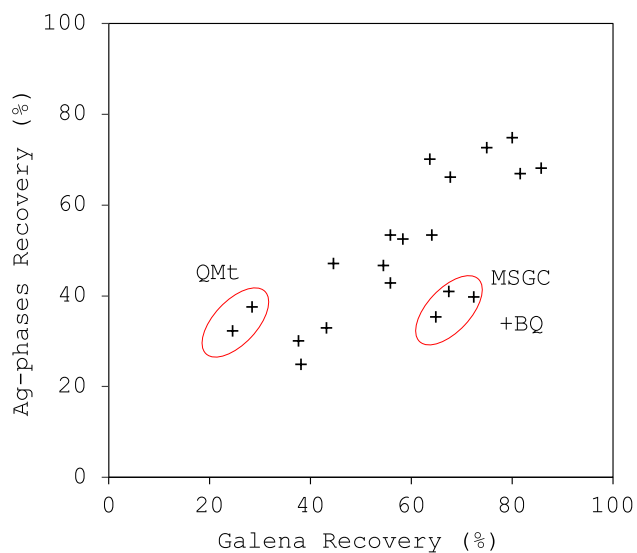
Fig. 11. Recovery for galena and Ag-phases. In red outlines are samples from QMt (quartz-magnetite), MSGC (massive sp-gn-py-ccp ± Au), and BQ (biotite-quartz-hosted ore). (For interpretation of the references to colour in this figure legend, the reader is referred to the web version of this article.)

compared to the Zn flotation can be attributed to the different mineral varieties targeted during the Cu-Pb flotation process. The Cu-Pb flotation circuit aims to recover various Cu-, Pb-, Ag-, and Au-bearing phases, which are comprised of a wide variety of minerals that occur from minor to trace amounts (Fig. 6). On the other hand, the Zn-flotation only targets sphalerite since gahnite, a zinc spinel ($ZnAl_2O_3$), is expected to report to the tailings. Sphalerite also occurs at a coarser grain size and a higher degree of liberation compared to galena, chalcopyrite, and other Ag-bearing phases (Fig. 7).

Between the different ore types, higher variability in grain size and degree of liberation is observed in galena, chalcopyrite, and Ag-bearing minerals than in sphalerite (Fig. 8 and Fig. 9). QMt, DOL, and MQ all show the lowest lead recovery values. DOL and MQ have the highest proportions of fine-grained galena ($P_{50} < 15$ μm) and the lowest mass proportions of liberated particles (<70 wt%). High copper recovery and grade in SKN samples can be attributed to coarser and more liberated chalcopyrite grains. The presence of coarser mineral grains will result in a higher degree of liberation for the same particle size distribution, which all else being equal, is expected to result in higher recovery (Gaudin et al., 1931). The poor performance of MnMSPG compared to other massive ore types is also possibly due to the relatively finer grain size of sphalerite and galena.

Talc-bearing ore (TLC) has relatively high zinc and lead recoveries similar to other massive ore types; however, concentrate grades are significantly lower (28% Pb and 54% Zn). At neutral pH and fine grain size (<50 μm), talc has the highest natural floatability (McHardy, 1973). pH was not controlled in the Cu-Pb flotation but was measured at pH 8 during the experiments. During the flotation test, the presence of talc also changed froth stability. Thus, higher dextrin concentration is needed to depress talc, which accounts for up to 5 wt% of the feed for TLC.
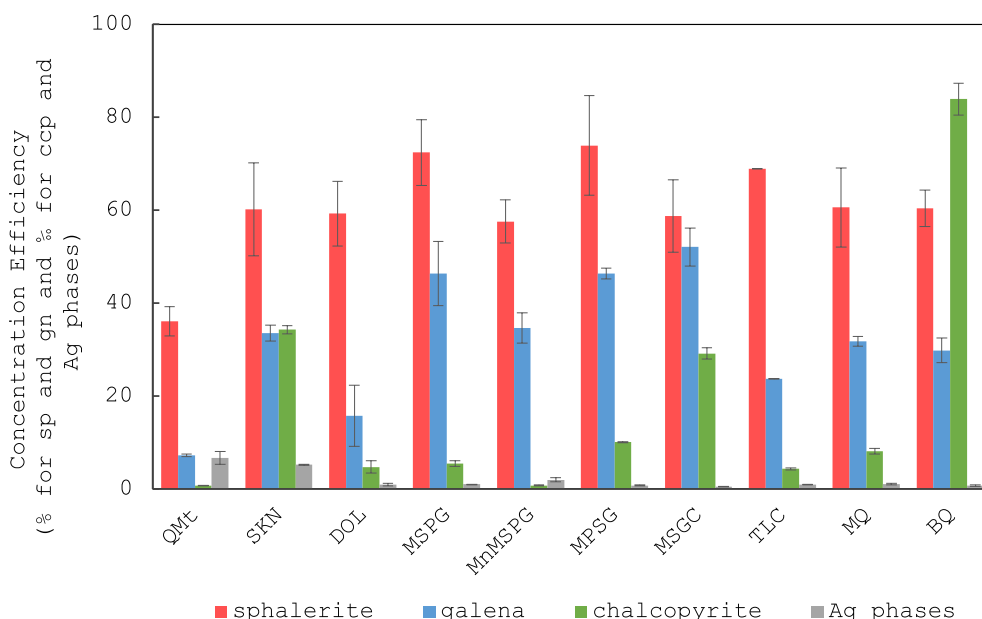
Fig. 12. Concentration efficiency (E_C) for sphalerite (in %), galena (in %), chalcopyrite (in ‰), and Ag-bearing phases (in ‰). Range bars indicate the values from the repeat flotation tests.
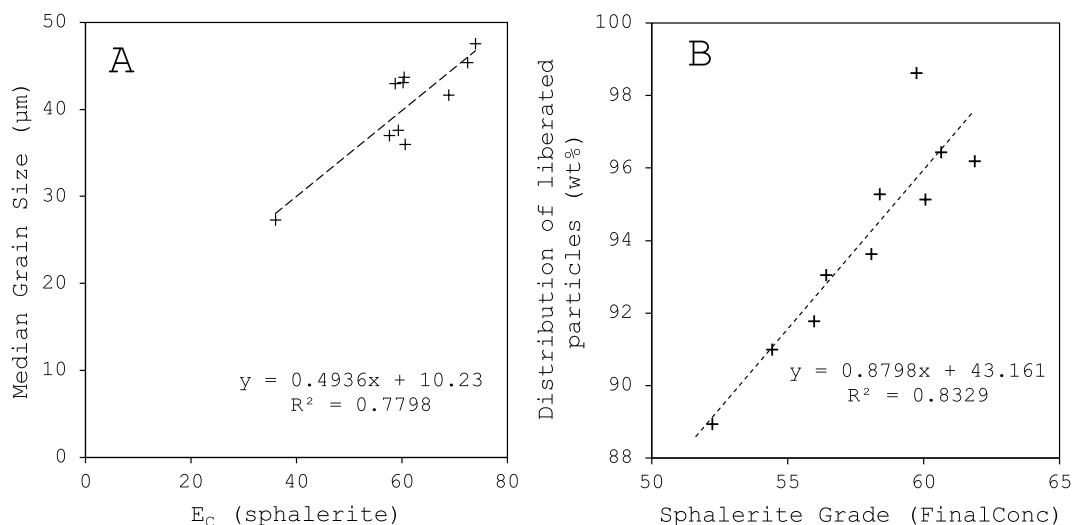
Table 5
One-way ANOVA results for the mean E_c values of the ten ore types for sphalerite, galena, chalcopyrite, and Au-Ag phases.

Phase	F-Value	p-Value
sphalerite	2.26	0.110
galena	15.17	<0.001
chalcopyrite	403.72	<0.001
Ag phases	21.01	<0.001

QMt distinctly differs from the other ore types, having the poorest flotation performance in terms of grade and recovery. Several factors contribute to this, including low sulfide content, poor liberation, finer grain size of sphalerite, galena, and chalcopyrite, and strong association of sulfides with pyrite and quartz. The high silica content (mainly quartz) of QMt samples makes this type of ore more challenging to grind and requires the highest energy requirement for the grinding process

(Stark, 2021). Despite these challenges, QMt exhibits the highest silver grade in the Cu-Pb concentrate due to the high amounts of silver minerals present in the feed. It also shows the highest liberation rates for Au-Ag phases (Fig. 9). However, silver recovery is low, ranging from 33% to 37%. This can be attributed to the presence of highly liberated extremely fine Ag-bearing particles (i.e.,P_{80} for Ag-phases is < 15 μm), which are harder to recover due to the low particle-bubble collision efficiency of fine particles in the conventional flotation process (Fuerstenau and Somasundaran, 2003). An example of a liberated Ag-rich electrum lost in the final tails is shown in Fig. 10A.

In addition, majority of the non-liberated Ag-bearing phases in QMt are associated with pyrite and quartz (e.g., Fig. 10B). Non-liberated Ag-bearing phases in other ore types are mainly associated with galena. Non-liberated Ag-bearing phases in coarser galena particles will have a higher probability to be recovered during Cu-Pb flotation than ultra-fine-grained liberated Ag-bearing phases. This trend is evident in Fig. 11, which shows that the recovery of galena is positively correlated

Fig. 13. (A) Plot of E_C values for sphalerite and the median grain size of sphalerite (ESD) and (B) plot of the final concentrate grade of sphalerite and the distribution of liberated sphalerite particles (>80% degree of liberation).

Table 6
Proposed geometallurgical domains for Lappberget.

Categories	Characteristics	Geometallurgical Domains	Geological Domains
Problematic ores	Poor selectivity	GM1	TLC
	Low-grade ores, fine-grained sulfides	GM2	DOL
		GM3	QMT*
Silver- and gold-rich ores	Complex silver mineralogy (high Ag concentrate grade)	GM4	SKN
	Gold-associated chalcopyrite-bearing ore (high Cu grade and recovery)	GM5	MSGC BQ*
Main sulfide ores	Disseminated sulfides	GM6	MQ*
	Massive sulfides	GM7	MSPG, MnMSPG, MPSG

* Quartz-rich rocks that require relatively higher energy for grinding.

with the recovery of Ag-bearing phases for most ore types. MSGC and BQ samples also deviate from the trend, possibly due to higher amounts of electrum, which are associated with chalcopyrite rather than galena (e. g., Fig. 10C and D).

3.3. Geometallurgical domains

Concentration efficiencies (E_c) of sphalerite, galena, chalcopyrite, and Ag-bearing phases were calculated to assess the metallurgical performance of each ore type in terms of selectivity and recovery. These are plotted in Fig. 12. Statistical analysis (ANOVA) was conducted based on the mean E_c values to determine if there are significant differences between the flotation performance of each ore type.

Based on the one-way ANOVA results (Table 5), there is no statistically significant difference between the mean E_c values for sphalerite between the different ore types (p-value > 0.05 at confidence level = 95%). However, when using Fisher's LSD method for pairwise comparisons of mean Ec values of sphalerite, it is clear that QMt stands out as having lower sphalerite recovery compared to the other ore types.

Despite this, the flotation behavior of sphalerite is similar across all ore types and is closely linked to the grain size and degree of liberation of the mineral. Fig. 13A shows a positive correlation between E_c and the median grain size of sphalerite. QMt ore, which has the lowest E_c value for sphalerite, has a distinctly low median sphalerite grain size of only 27 μm. The sphalerite grade in the final zinc concentrate strongly correlates with the number of liberated particles in the sample, as shown in Fig. 13B. Fully liberated particles are considered fast-floating fractions that are quickly recovered during the cleaning stages (Jameson, 2012; Jameson et al., 1977). The significant effect of grain size and degree of liberation on sphalerite flotation was also observed from the particle-based modeling by Tiu et al. (2022).

Unlike sphalerite, the calculated mean E_c values for chalcopyrite, galena, and Ag-bearing phases for the different ore types showed significant differences (p-value ≪0.05 at confidence level = 95% (Table 5)). The high F-value for chalcopyrite suggests a high variability between the flotation performance of the different ore types. This is mainly due to the high E_c values for Cu-rich ores BQ, MSGC, and SKN. Low E_c values for galena are recorded for TLC, DOL, and QMT. In terms of Ag-bearing phases, QMt and SKN have higher mean E_c values due to the high silver grade in the feed. Other ore types do not show significant differences in mean E_c values.

Based on these results, the ore types can be simplified into seven geometallurgical domains, as listed in Table 6. The domains are categorized as: (1) problematic ores, (2) silver- and gold-rich ores, and (3) main sulfide ores. Problematic ores are domains that gave the poorest flotation performance during the Cu-Pb flotation (and Zn-flotation for QMt). This is mainly due to the mineralogical and textural characteristics of the ores. Problematic ores can be blended with other ore types to improve its recovery or avoid penalties. For example, TLC ores can be blended with other types to minimize the introduction of talc in the flotation process. These ores can also undergo de-sliming to remove some of the talc before flotation.

Silver- and gold-rich ores are economically attractive due to the high content of precious metals. The silver-rich ores GM3 and GM4 are found at the upper part of the deposit, whereas the gold-rich ore GM5 occurs at depth. The complex mineralogy and occurrence of silver on these types
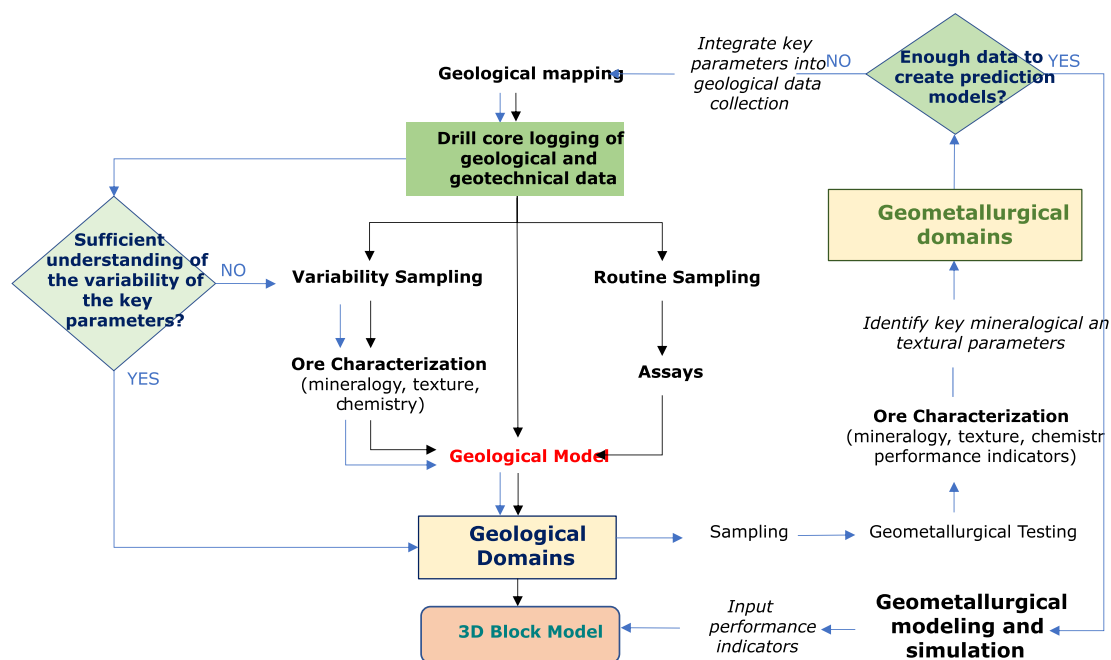
Fig. 14. Proposed geometallurgical approach for defining geometallurgical domains. Black lines follow the normal route in creating geological domains, whereas blue lines provide the route to defining the geometallurgical domains from the geological data. (For interpretation of the references to colour in this figure legend, the reader is referred to the web version of this article.)

of ores can also lead to poor recovery despite having higher silver feed grades (e.g., fine-grain and complex intergrowth with pyrite in QMt). GM3 and GM4 are also associated with higher antimony and arsenic content due to relatively high amounts of sulfosalts. To improve the recovery of silver and gold, further work should also focus on optimizing the gravimetric circuit.

The third category, the main sulfide ores, refers to sphalerite-rich ores that are characteristic of the main ore lenses in the Lappberget ore body. There is no significant difference between the flotation performance of GM6 and GM7. However, GM6 is expected to have lower grindability performance due to its high quartz content (Stark, 2021).

4. Proposed approach for geometallurgical characterization

A geometallurgical approach for characterization is proposed based on the methodology and results of this study, as illustrated in Fig. 14. This is best suited for pre-feasibility and feasibility studies. This approach mainly focuses on using pre-defined geological domains as 'seed' domains, especially when dealing with complex ores. The geologically constrained domains reflect the different ore forming conditions, which results to the natural heterogeneity of the ore in terms of mineralogy and texture.

It is crucial to identify key mineralogical and textural parameters in the process performance (e.g., presence of talc, Au-rich zones) during the first iteration process. Geometallurgical domains can be established based on the distinct metallurgical performance of the ore types related to their geological characteristics. If sufficient information has been acquired to create prediction models, geometallurgical modeling and simulation can be conducted to calculate key performance indicators (e. g., grade and recovery, Net Smelter Return), which can be integrated into the 3D block model. Otherwise, the key mineralogical and textural parameters identified should be integrated into the geological data collection. These parameters must be logged in a quantifiable matter to sufficiently provide data for the prediction models.

It is important to note that this geometallurgical approach is a continuous process, and as more data is collected and analyzed, the prediction models can be refined and updated to improve their accuracy. This process is repeated until sufficient data is acquired to create a robust geometallurgical model for the entire deposit. This approach will help better guide geological data acquisition to gear toward process-related parameters, effectively optimizing data collection from a geological and process performance perspective.

5. Conclusion and recommendations

The variability in the flotation performance of the different ore types in the Lappberget Zn-Pb-Ag-(Cu-Au) deposit can be attributed to the complex mineralogy and texture present in the deposit. Mineralogy, mineral chemistry, grain size, degree of liberation, and mineral associations are key contributing factors affecting the variability in the performance of the ore. The effect of each factor varies depending on the characteristics of the target mineral(s) and the complexity of their association with other minerals. The significance of grain size and degree of liberation on the flotation performance suggests that geometallurgical models should include texture as a critical input variable to accurately predict flotation performance. The complex mineralogy, fine grain size, and complex intergrowth of Cu-, Au-, and Ag-bearing minerals for the different ore types lead to poor liberation. The strong association of Cu- and Ag-bearing minerals with galena for some ore types leads to higher recovery in the Cu-Pb flotation despite poor liberation rates. Due to the high variability of the flotation performance during the Cu-Pb flotation, further research should focus on identifying and validating the correlations between the mineralogical and textural characteristics and the metallurgical response for the different geometallurgical domains. Additional research should explore the correlation between equipment- and operation-related factors and flotation performance using processing plant samples. This extension from laboratory tests to plant conditions will enhance the study's findings. Furthermore, it is also crucial to investigate the behavior of different ore types in various beneficiation processes, including comminution, gravity separation, and classification.

The proposed geometallurgical approach for characterization is particularly effective in characterizing complex ores, such as the polymetallic Lappberget Zn-Pb-Ag-(Cu-Au) deposit at the Garpenberg mine. By relating the geological characteristics, such as mineralogy and textures, to the metallurgical performance, this approach can provide a comprehensive understanding of the variability in flotation performance within the deposit. With sufficient data, the approach can be used to develop predictive recovery models that can be incorporated into geometallurgical modeling and simulation of the entire deposit, allowing for more accurate forecasting of plant performance and recoveries.

CRediT authorship contribution statement

Glacialle Tiu: Conceptualization, Data curation, Formal analysis, Investigation, Methodology, Writing – original draft, Validation, Visualization. **Yousef Ghorbani:** Methodology, Writing – review & editing, Supervision. **Nils Jansson:** Methodology, Writing – review & editing, Supervision. **Christina Wanhainen:** Conceptualization, Methodology, Writing – review & editing, Supervision, Funding acquisition, Resources, Project administration. **Nils-Johan Bolin:** Conceptualization, Methodology, Writing – review & editing.

Declaration of Competing Interest

The authors declare that they have no known competing financial interests or personal relationships that could have appeared to influence the work reported in this paper.

Data availability

Data will be made available on request.

Acknowledgments

Appendix A. Supplementary data

Supplementary data to this article can be found online at https://doi.org/10.1016/j.mineng.2023.108323.

References

Allen, R.L., Bull, S., Ripa, M., Jonsson, R., 2003. Regional stratigraphy, basin evolution, and the setting of stratabound Zn-Pb-Cu-Ag-Au deposits in Bergslagen. Final report for Boliden Mineral and SGU-FoU project 03–1203/99, Sweden.

Alruiz, O.M., Morrell, S., Suazo, C.J., Naranjo, A., 2009. A novel approach to the geometallurgical modelling of the Collahuasi grinding circuit. Minerals Engineering 22, 1060–1067. https://doi.org/10.1016/j.mineng.2009.03.017.

Bahrami, A., Ghorbani, Y., Sharif, J.A., Kazemi, F., Abdollahi, M., Salahshur, A., Danesh, A., 2021. A geometallurgical study of flotation performance in supergene and hypogene zones of Sungun copper deposit. Miner. Process. Extr. Metall. Trans. Inst. Min. Metall. 130, 126–135. https://doi.org/10.1080/25726641.2019.1591794.

Bevandic, S., 2022. Geometallurgical characterisation of Zn-Pb mine waste in view of (near) zero-waste valorisation. KU Leuven, Plombières, East Belgium.

Boroh, A.W., Sore-Gamo, K.Y., Ayiwouo, N., Gbambie, M., Ngounouno, I., 2021. Implication of geological domains data for modeling and estimating resources from Nkout iron deposit (South-Cameroun). J. Min. Metall. A Min. 57 (1), 1–17.

Derrien, M., 2022. Boliden Summary Report: Mineral Resources and Mineral Reserves 2021 Garpenberg.

Diamond, R.W., Trail, B.C., 1927. Ore concentration practice of the consolidated mining & smelting Co. of canada, Ltd. Transactions of AIME 9, 95–106.

Ehrig, K., Liebezeit, V., Smith, M., Macmillan, E., Lower, C., 2014. Geologists and the Value Chain – How Material Characterisation by Modern Mineralogy can Optimise Design and Operation of Processing Facilities, in: 9th International Mining Geology Conference, Adelaide, 18-20 August 2014. pp. 5–13.

Fuerstenau, M.C., Somasundaran, P., 2003. Flotation. In: Fuerstenau, M.C., Han, K.N. (Eds.), Principies of Mineral Processing. SME, Littleton, pp. 245–306.

Gaudin, A.M., Butte, M., 1930. Selectivity index; A yardstick of the segregation accomplished by concentrating operations. Transactions of AIME 87, 483–487.

Gaudin, A.M., Groh, J.O., Henderson, H.B., 1931. Effect of particle size on flotation. Am. Inst. Min. Metall. Eng. Tech. Publi 414, 3–23.

Gordon, H.J.J., 2019. A mineralogical approach to quantifying ore variability within a polymetallic Cu-Pb-Zn Broken Hill-type deposit and its implications for geometallurgy. Stellenbosch University.

Gottlieb, P., Wilkie, G., Sutherland, D., Ho-Tun, E., Suthers, S., Perera, K., Jenkins, B., Spencer, S., Butcher, A., Rayner, J., 2000. Using quantitative electron microscopy for process mineralogy applications. JOM 52 (4), 24–25. https://doi.org/10.1007/s11837-000-0126-9.

Intertek, 2020. Mineral Services: Schedule of Services and Charges Australia.

Jameson, G.J., 2012. The effect of surface liberation and particle size on flotation rate constants. Minerals Engineering 36–38, 132–137. https://doi.org/10.1016/j.mineng.2012.03.011.

Jameson, G.J., Nam, S., Moo Young, M., 1977. Physical factors affecting recovery rates in flotation. Min. Sci Eng 9, 103–118.

Jansson, N.F., Allen, R.L., 2011. Timing of volcanism, hydrothermal alteration and ore formation at garpenberg. Bergslagen, Sweden Gff 133, 3–18. https://doi.org/10.1080/11035897.2010.547597.

Johnson, N.W., Munro, P.D., 2008. Methods for assigning domains in the primary sulfide zone of a sulfide orebody, in. In: Proceedings of the Ninth International Congress for Applied Mineralogy, pp. 597–603.

Kopacz, M., Kulpa, J., Galica, D., Olczak, P., 2020. The influence of variability models for selected geological parameters on the resource base and economic efficiency measures - Example of coking coal deposit. Resources Policy 68, 101711.

Lamberg, P., Rosenkranz, J., Wanhainen, C., Lund, C., Minz, F., Mwanga, A., Parian, M., 2013. Building a geometallurgical model in iron ores using a mineralogical approach with liberation data. Building a Geometallurgical Model in Iron Ores Using a Mineralogical Approach with Liberation Data. 317–324.

Lishchuk, V., Koch, P.H., Ghorbani, Y., Butcher, A.R., 2020. Towards integrated geometallurgical approach: Critical review of current practices and future trends. Minerals Engineering106072 145. https://doi.org/10.1016/j.mineng.2019.106072.

Lishchuk, V., 2016. Geometallurgical Programs – Critical Evaluation of Applied Methods and Techniques.

Lund, C., 2013. Mineralogical, chemical and textural characterisation of the Malmberget iron ore deposit for a geometallurgical model. Luleå University of Technology. PhD Thesis.

Luyken, W., Bierbrauer, E., 1929. Calculations in Ore Dressing. Trans. AIME 214, 25.

Martino, R., de Araujo, A.C., Barbosa, M.G., Gaydardzhiev, S., 2016. Geometallurgical modelling of low-grade itabirite iron ores from the iron quadrangle, Brazil, in: IMPC 2016 - 28th International Mineral Processing Congress. pp. 1–10.

McHardy, J.C., 1973. Surface chemistry of talc flotation. McGill university.

Minz, F., Bolin, N.J., Lamberg, P., Wanhainen, C., 2013. Detailed characterisation of antimony mineralogy in a geometallurgical context at the Rockliden ore deposit, north-central sweden. Minerals Engineering 52, 95–103. https://doi.org/10.1016/j.mineng.2013.04.017.

Olarewaju, A.O., Ayodele, B.E., Gbenga, B.S., 2015. Geometallurgical evaluation of itapa ekiti feldspathic-biotite ore deposit for effective processing and extraction. Int. J. Min. Eng. Miner. Process. 4, 1–7. https://doi.org/10.5923/j.mining.20150401.01.

Rajabinasab, B., Asghari, O., 2019. Geometallurgical domaining by cluster analysis: Iron ore deposit case study. Natural Resources Research 28, 665–684. https://doi.org/10.1007/s11053-018-9411-6.

Spleit, M., Dimitrakopoulos, R., 2017. Modelling geological variability in the LabMag iron ore deposit and effects on the long-term production schedule. Trans. Institutions Min Metall. Sect. A Min. Technol. 126, 44–58. https://doi.org/10.1080/14749009.2016.1235247.

Stark, G.L., 2021. A process mineralogy study of grinding characteristics for the polymetallic orebody. Luleå University of Technology, Lappberget Garpenberg.

Stevens, J.R., Collins, D.M., 1961. The technical efficiency of concentration operations. Q. Color. Sch. Mines 56, 483–508.

Suazo, C.J., Kracht, W., Alruiz, O.M., 2010. Geometallurgical modelling of the Collahuasi flotation circuit. Minerals Engineering 23, 137–142. https://doi.org/10.1016/j.mineng.2009.11.005.

Tijsseling, L.T., Dehaine, Q., Rollinson, G.K., Glass, H.J., 2020. Mineralogical prediction of flotation performance for a sediment-hosted copper–cobalt sulphide ore. Minerals 10, 1–21. https://doi.org/10.3390/min10050474.

Tiu, G., Jansson, N., Wanhainen, C., Ghorbani, Y., Lilja, L., 2021. Ore mineralogy and trace element (re)distribution at the metamorphosed Lappberget Zn-Pb-Ag-(Cu-Au) deposit, Garpenberg. Sweden. Ore Geol. Rev. 135, 104223. https://doi.org/10.1016/j.oregeorev.2021.104223.

Tiu, G., Ghorbani, Y., Jansson, N., Wanhainen, C., Bolin, N.-J., 2022. Ore mineral characteristics as rate-limiting factors in sphalerite flotation: Comparison of the mineral chemistry (iron and manganese content), grain size, and liberation. Minerals Engineering 185, 107705. https://doi.org/10.1016/j.mineng.2022.107705.

Triola, M., 2018. Minitab® Manual, 13th ed. Pearson Education.

Whiten, B., 2007. Calculation of mineral composition from chemical assays. Mineral Processing and Extractive Metallurgy Review 29, 83–97. https://doi.org/10.1080/08827500701257860.

Williams, S.R., Richardson, J.M., 2004. Geometallurgical mapping: A new approach that reduces technical risk geometallurgical mapping. SGS Miner. Serv. 1–13.